PHYSICAL REVIEW B VOLUME 24, NUMBER 11 1 DECEMBER 1981

Zero-phonon structures in the optical spectra of some transition-metal ions in CdSe crystals

D. Buhmann, H.-J. Schulz, and M. Thiede
Fritz-Haber-Institut der Max-Planck-Gesellschaft, Elektronenmikroskopie
Faradayweg 4-6, 1000 Berlin 33, Germany
(Received 1 December 1980)

Zero-phonon structures of the Fe^{2+} $3d^6$ $^5E(D) \leftrightarrow {}^5T_2(D)$ transition in absorption and emission include a coinciding line at 2376 cm^{-1}. Polarized transmission spectra of the Co^{2+} $3d^7$ transition $^4A_2(F) \rightarrow {}^4T_1(P)$ display components split by second-order spin-orbit coupling and indicate an autoionization effect at the 14 175-cm^{-1} line. Symmetry arguments support the interpretation of this antiresonance by a $Co^{2+} \rightarrow Co^{3+}$ charge-transfer process with a threshold at about 13 800 cm^{-1}. The $^4T_2(F) \rightarrow {}^4A_2(F)$ luminescence transition of Co^{2+} gives rise to a zero-phonon line at 2867 cm^{-1}. The fine structure of the $^3T_1(F) \rightarrow {}^3T_1(P)$ absorption of Ni^{2+} $3d^8$ suggests a strong reduction of spin-orbit coupling by the Jahn-Teller interaction. With Ni^{2+} ions, radiative recombination from the $^3T_1(P)$, $^3A_2(F)$, and $^3T_2(F)$ levels to the $^3T_1$ ground state is detected, and the first and the last transitions exhibit zero-phonon lines at 10 926 and 3607 cm^{-1}, respectively. An abundant novel emission band characterized by a zero-phonon transition at 10 170 cm^{-1} may be related to an M center, i.e., a $(V_{Se}^{-} V_{Se}^{-})^{2+}$ associated defect.

I. INTRODUCTION

Among the II-VI semiconductors, cadmium selenide has, up to now, received less attention than most other members of this family of compounds as far as research on optical properties is concerned. This may be partly due to the fact that the band gap of CdSe correcponds to the low-energy end of the visible spectrum so that infrared techniques are necessary to study its behavior in the transmission range. In view of its increasing importance for applications, e.g., in the production of thin-film solar cells, however, it seems safe to forecast an increasing demand for precise data on the optical properties of this material.

In this paper new results are reported on a number of impurities in CdSe. Absorption and emission measurements at low temperatures ($2\,K \leq T \leq 5$ K) supply further information on absorption properties of transition metals in CdSe, as reported by Langer and Baranowski[1] for $T = 80$ K, and additionally on their emission behavior. In particular, distinct zero-phonon structures have been found for several impurities. At two of the Ni^{2+} transitions, viz. $^3T_1(F) \leftrightarrow {}^3T_1(P)$ and $^3T_1(F) \leftrightarrow {}^3T_2(F)$, and at the Fe^{2+} transition $^5E(D) \leftrightarrow {}^5T_2(D)$, the zero-phonon lines coappeared in absorption and emission. The emission spectra, apart from the vanadium emission, are reported for the first time.

II. EXPERIMENTAL TECHNIQUE

The experimental arrangements were conventional in both emission and absorption. An evacuated spectrometer (Jarrell-Ash, 1 m focal length) with various gratings was used to cover the spectral region extending from the visible range to $\lambda \cong 4.5$ μm. The imaging beam path before and behind the monochromator could also be guided in vacuum. This was particularly advantageous for measurements in the middle-infrared region where otherwise disturbing atmospheric absorptions occur. The specimens were cooled in a helium immersion cryostat so that they could be investigated at temperatures from 2.0 to 4.2 K. In absorption experiments, either a tungsten-halogen lamp or a globar were employed as a light source. For the excitation of luminescence mostly a xenon high-pressure lamp with suitable filters was used, or sometimes an argon laser with 1 W output instead ($\lambda = 514.5$ nm, i.e., $\bar{\nu} = 19\,440$ cm^{-1}).

As detectors, cooled photomultipliers with an $S1$ cathode and cooled PbS or PbSe photoresistors or an InSb diode were applied. Owing to the restrict-

ed spectral ranges and the often rather sharp structures in the spectra, a correction of the spectra with regard to the spectral response of the respective detector and the grating efficiency could, in general, be avoided. The electric signals were processed by means of lock-in technique.

The investigated crystals were partly grown from the vapor phase and partly from the melt; they were investigated either as-grown or after being sawed into small pieces and being surface polished. The crystals were partly doped intentionally with vanadium or nickel; other crystals such as the Co-doped crystal, were only accidentally doped so that the transitions observed with them were mostly weak, however, well structured due to the low-impurity concentrations. The doping with vanadium was carried out by vapor deposition of purified vanadium onto the crystal and subsequent annealing of several hours at $T=900\,^{\circ}\mathrm{C}$ in vacuum; nickel doping was effected by adding nickel to the starting material before growing the crystal.

III. RESULTS OF MEASUREMENTS AND DISCUSSION

A. Iron (Fe^{2+})

The transition ${}^5E(D) \leftrightarrow {}^5T_2(D)$ of the Fe^{2+} ion ($3d^6$ configuration) was discovered in absorption[1] in the spectral range around 2500 cm^{-1}. At $T=8$ K the authors of Ref. 1 recorded the rising point of the absorption band near $\bar{\nu} \simeq 2260$ cm^{-1} as well as further structures in the following range of higher photon energies up to about 3500 cm^{-1}.

This absorption is investigated in detail in this paper and, for the first time, an emission of the Fe^{2+} ion in CdSe is detected at $T \simeq 4$ K. This emission can be identified by coincidence of the zero-phonon transition at 2375 cm^{-1} with the narrow line in the well-resolved fine-structure spectrum in absorption (Fig. 1 and Table I). Here, the absorption starts with the transition at 2376 cm^{-1} and displays satellites at 2391 and 2420 cm^{-1}. The latter satellite has a distance of 44 cm^{-1} from the zero-phonon line (ZPL); the emission also displays a broad satellite in nearly the same distance, that is at 2330 cm^{-1}. The emission displays here only three electronic transitions whereas for ZnS:Fe^{2+} four transitions are found, two of which have a doublet structure (cf. Ref. 2). Though this doublet splitting at ZnSe:Fe^{2+} is of similar magnitude as the splitting in our 2357-2363 cm^{-1} doublet, a self-absorption is probably the cause there,

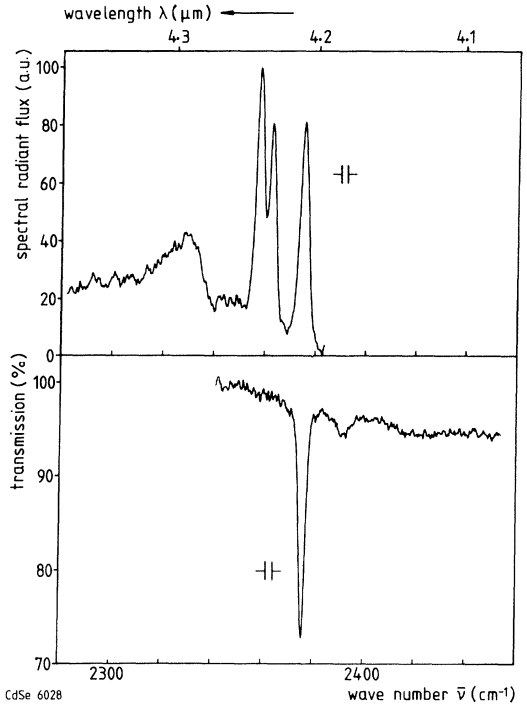

FIG. 1. Emission and transmission spectrum of a CdSe:Fe^{2+} crystal (no. 6028) at $T \simeq 4$ K: ${}^5E(D) \leftrightarrow {}^5T_2(D)$ transition. Excitation range in the emission experiment: 7500 $cm^{-1} \lesssim \bar{\nu} \lesssim 15\,000$ cm^{-1}. Grating blazed at 3850 cm^{-1}, cooled PbSe detector with Ge filter. Emission averaged over 10 scans.

whereas in our case self-absorption can be fairly well excluded.

The fine structure shown could only be displayed due to the possibility of evacuating the beam path, because there are strong disturbing CO_2 absorption bands in the 2400-cm^{-1} range. It is, therefore, assumed that the authors of Ref. 1 did not recognize residua of such influences in their spectra and that their absorption structure at $\bar{\nu} < 2300$ cm^{-1} is mistaken.

Low and Weger[3] calculated the splitting of the ${}^5E(D)$ ground term of d^6 in a tetrahedral crystal field, including second-order spin-orbit coupling. They obtained an equidistant quintet of the spacing $6\lambda^2/\Delta$, with the spin-orbit coupling parameter λ and the crystal field parameter $\Delta = 10Dq$. With a Γ_5 component of the ${}^5T_2(D)$ upper term being lowest, and taking into account that in T_d $\Gamma_5 \leftrightarrow \Gamma_2$ is forbidden as an electric dipole transition, four lines can be expected in emission, the one with highest energy coinciding with the single absorption line at very low temperatures. This is indeed the situation observed with cubic ZnS:Fe^{2+}.[4,5,2] Adopting the same splitting pattern for CdSe in

TABLE I. Detected optical transitions in absorption ($T \simeq 2$ K) and emission ($T \simeq 4.2$ K) with four different centers in CdSe. The assignments of the transitions are given as based on crystal-field theory for T_d symmetry, with inclusion of spin-orbit coupling where appropriate. All wave numbers in cm^{-1}. Zero-phonon transitions are underlined.

Center	Absorption	Emission	Transition
Fe^{2+}		2330	
		<u>2357</u>	Γ_5-$^5T_2(D) \rightarrow \Gamma_5$-$^5E(D)$
		<u>2363</u>	Γ_5-$^5T_2(D) \rightarrow \Gamma_3$-$^5E(D)$
	<u>2376</u>	<u>2375</u>	Γ_5-$^5T_2(D) \rightarrow \Gamma_1$-$^5E(D)$
	2391		
	2420		
Co^{2+}		2654	ZPL − LO
		2826	
		<u>2867</u>	$^4T_2(F) \rightarrow {}^4A_2(F)$
	<u>12 788</u>		Γ_8-$^4A_2(F) \rightarrow \Gamma_8$-$^4T_1(P)$
	<u>12 859</u>		Γ_8-$^4A_2(F) \rightarrow \Gamma_7$-$^4T_1(P)$
	12 993		ZPL + LO
	13 060		ZPL + LO
	<u>13 422</u>		Γ_8-$^4A_2(F) \rightarrow \Gamma_8$-$^4T_1(P)$
	13 502		
	13 550		
	13 620		ZPL + LO
	<u>14 175</u>		Γ_8-$^4A_2(F) \rightarrow \Gamma_6$-$^4T_1(P)$
V^{3+}		4300	$^3T_2(F) \rightarrow {}^3A_2(F)$
Intrinsic		9893	
defect		9950	ZPL − LO
		10 019	ZPL − TO
		10 070	
		10 120	
		<u>10 170</u>	ZPL

cubic approximation, an additional mechanism has to be assumed by which an expected emission line near $\bar{\nu} = 2369$ cm^{-1} would be quenched. As depicted above, $\Delta = 2400$ cm^{-1} would then imply $\lambda \simeq 48$ cm^{-1}, i.e., approximately a 50% reduction versus the free-ion value.

If we compare the Fe^{2+} emission spectrum for crystals with different Fe concentrations (Fig. 2, here always accidental doping) we can see that the zero-phonon structures decrease, in relation to the phonon sideband, with increasing coupling of the electronic transition to the lattice. Since an increasing strength in the zero-phonon lines with decreasing doping had been demonstrated[2] with ZnS:Cr^{2+} and ZnS:Fe^{2+}, a transfer of this conclusion would imply increasing Fe^{2+} concentration in our crystal sequence nos. 6028, 6015, 6029, and 35.

One might be tempted to relate the remarkable "antiresonance" in the emission spectrum of Fig. 1 to the low-temperature behavior of the thermal conductivity of iron-doped II-VI compounds.[6] For some of these materials, a resonant one-phonon scattering mechanism has been established which involves the spin-orbit components of the Fe^{2+} ground state. Although for ZnS:Fe^{2+} the resonant scattering proved to be most pronounced for temperatures well above $T \cong 4$ K,[7] the small spin-orbit splitting of only 6 cm^{-1} found here with CdSe may account for the specific properties of Fe^{2+} in this very material. Since both E and T_2 mode distortions of the tetrahedral iron cluster are important for one-phonon transitions commencing from the Γ_4-type second energy level of the five components of the orbital E state,[6] a detailed treatment of the processes which are allowed under the selection rules for this impurity-lattice coupling may lead to the conditions which invoke the apparent

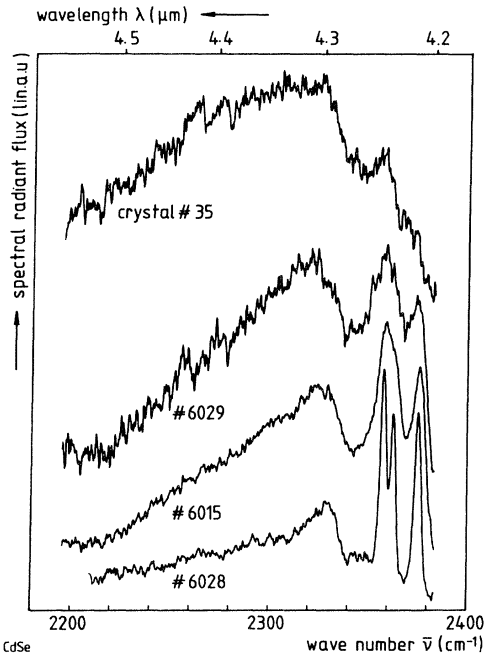

FIG. 2. Luminescence of four CdSe:Fe^{2+} crystals with different unknown concentrations of iron at $T \cong 4$ K. Zero lines have been shifted to avoid overlap between spectra. Spectral slit width $\Delta\bar{\nu}=3$ cm^{-1}, except for crystal no. 35, where it was 6 cm^{-1}.

quenching of emission transitions terminating in this particular level. While Fig. 2 indicates that the Fe^{2+} concentration has no influence on the vanishing of this Γ_5 $({}^5T_2)\rightarrow\Gamma_4$ $({}^5E)$ transition, the temperature dependence of the emission spectrum is expected to yield additional evidence for the proposed interaction. These measurements and experiments on the low-temperature thermal conductivity of these samples are in preparation here.

B. Cobalt (Co^{2+})

Among the known Co^{2+} $3d^7$ absorption bands,[1] because of the low Co-doping, mainly the strongest transition ${}^4A_2(F)\rightarrow{}^4T_1(P)$ has been investigated here for reasons of intensity. At $T=2$ K zero-phonon transitions could be resolved, cf. Fig. 3. Three groups of absorption transitions can be distinguished in this range: near $\bar{\nu}\simeq 12\,800$, 13 400, and 14 200 cm^{-1}. This triplet structure was observed by Langer and Baranowski[1] at $T=80$ K; the splitting has been assigned to first-order spin-orbit coupling at ${}^4T_1(P)$ (see level scheme in Fig. 3).

The triplet transition of smallest energy Γ_8-${}^4A_2(F)\rightarrow\Gamma_7,\Gamma_8$-${}^4T_1(P)$ is further split by second-order spin-orbit coupling; the observed doublet spacing is $\Delta\bar{\nu}=71$ cm^{-1} (cf. Table I). [If spin-orbit coupling is considered, the energy levels are classified according to the irreducible representations of the double group $\bar{T}_d$ which are here named Γ_i (after Ref. 8).] The doublet is repeated in a blurred manner near $\bar{\nu}\simeq 13\,000$ cm^{-1}, i.e., displaced by one LO phonon energy. These satellites, as some other structures to be dealt with, are hardly discernible in Fig. 3 because of the broad energy range depicted but they can safely be identified in a scan of a narrow region.

The next higher triplet transition at $\bar{\nu}=13\,400$ cm^{-1}, i.e., Γ_8-${}^4A_2(F)\rightarrow\Gamma_8$-${}^4T_1(P)$, displays only one zero-phonon line, corresponding with the Co^{2+} model. The secondary maxima occur in distances of 80, 128, and 198 cm^{-1} from the ZPL and can be ascribed to coupling with lattice vibrations; some of the noted energy differences do not, however, agree with phonons of the CdSe host lattice (cf. Table II).

The transition of highest energy, i.e., Γ_8-${}^4A_2(F)$ $\rightarrow\Gamma_6$-${}^4T_1(P)$ at $\bar{\nu}\simeq 14\,175$ cm^{-1}, displays a peculiarity as to its polarization behavior; moreover, only one individual line occurs without any phonon satellites. For $\vec{E}\|c$ the spectrum shows a pronounced absorption line whereas for $\vec{E}\perp c$ the line appears as a negative absorption at the same place.

Donor-acceptor pairs could, possibly, be involved in this effect, since their zero-phonon transitions could be situated in this energy range.[9,10] Yet charge-transfer transitions are also apt to intervene here in the vicinity of the band edge. The position of cobalt centers in the energy gap has recently been determined for a number of II-VI semiconductors.[11] Since Radlinski could not detect an ir luminescence of Co^{2+} in CdSe, however, his conclusion[11] on the ground-state position is based on a false presumption in this case.

The consideration of charge-transfer processes leads to a most tempting explanation of the "negative absorption," that is, the potentiality of an antiresonance.[12] This effect, which corresponds to the autoionization in atomic physics, would occur if a discrete state is degenerate with a continuum of states. Indications of Co^{2+} excitation levels with $\bar{\nu}<10\,100$ cm^{-1} (at $T\simeq 80$ K) in CdSe being degenerate with the conduction band have been derived earlier[13] from photoconductivity spectra. We therefore imagine the "positive dip" in the $\vec{E}\perp c$ spectrum of Fig. 3 to be correlated with this type

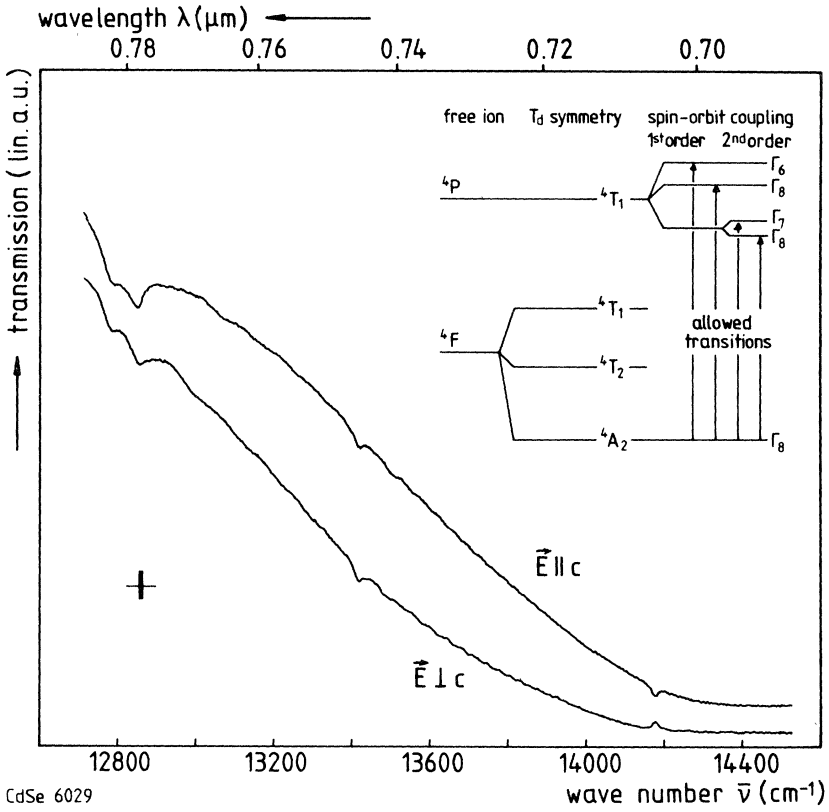

FIG. 3. Transmission spectrum of a CdSe:Co^{2+} crystal (no. 6029) at $T \cong 2$ K for two orientations of the incident light $\vec{E}$ vector with respect to the c axis of the crystal. Zero lines have been shifted to avoid overlap between spectra. Each of the spectra covers approximately the range of 0 to 90% transmission. Inset: Relevant part of the splitting scheme of the energy levels of the $3d^7$ electron configuration in a tetrahedral crystal field. Grating blazed near 6200 cm^{-1}, used in second order. Cooled photomultiplier with $S1$-type cathode (EMI 9684B).

of interaction. It is interesting to note that the spectral position of this transition is slightly varying for different crystals. This observation may be related to distortions of the charge-transfer band with changing cobalt concentration.

The most striking feature of the antiresonance is its absence in one polarization direction. Since the rest of the splitting behavior of the Co^{2+} levels is explicable by means of a T_d crystal field, it is likely that the C_{6v} band structure of the host lattice is here involved in the form of a symmetry selection rule. To advance such a relation, we assume a local C_{3v} symmetry for the environment of the ion and take the compatibility between T_d (Co^{2+} ion

TABLE II. Some characteristic phonon energies of the CdSe lattice.

Designation	$\frac{\hbar\omega}{hc}$ (cm^{-1})	Reference
TA	60	Geick *et al.*[16] 1966
LA	110	Geick *et al.*[16] 1966
TO	155	Geick *et al.*[16] 1966
TO(∥)	166	Beserman[17] 1969; Plotnichenko *et al.*[18] 1977
TO(⊥)	169,171	Beserman[17] 1969; Plotnichenko *et al.*[18] 1977
LO	196	Fukumoto *et al.*[19] 1972
LO	200	Geick *et al.*[16] 1966
LO(∥,⊥)	209–212	Plotnichenko *et al.*[18] 1977 Beserman[17] 1969; Yu[20] 1976

with its next-nearest neighbors) and C_{6v} (CdSe lattice) into account. In principle, there are two different possibilities for a charge-transfer process at the Co^{2+} ion:

$$\text{(i) } Co^{2+}\, d^7 + h\nu \rightarrow Co^{3+} d^6 + e^-_{CB} \,,$$

$$\text{(ii) } Co^{2+} d^7 + e^-_{VB} + h\nu \rightarrow Co^{+}\, d^8 \,.$$

In the notation of Ref. 8, for the irreducible representations of the double group $\bar{C}_{3v}$, the electric dipole moment operator transforms in this group according to Γ_1 for $\vec{E}||c$ and as Γ_3 for $\vec{E}\perp c$. In process (i), the ground state of Co^{2+} and the conduction-band (CB) minimum are involved, hence we allow for the compatibility relations:

$$Co^{2+}: \ \Gamma_8(\bar{T}_d) \rightarrow \Gamma_4 + \Gamma_5 + \Gamma_6(\bar{C}_{3v})$$

and

$$CB: \ \Gamma_7(\bar{C}_{6v}) \rightarrow \Gamma_4(\bar{C}_{3v}) \,.$$

Correspondingly, for process (ii) we take into account (VB denotes valence band):

$$VB: \ \Gamma_9(\bar{C}_{6v}) \rightarrow \Gamma_5 + \Gamma_6(\bar{C}_{3v})$$

and

$$Co^{+}: \ \Gamma_1(\bar{C}_{3v}) \,.$$

By forming the relevant inner Kronecker products of the noted irreducible representations, the transition (ii) proves to be forbidden for both $\vec{E}||c$ and $\vec{E}\perp c$. On the other hand, process (i) is symmetry allowed from Γ_4 for both polarization directions but from the Kramer's doublet Γ_5, Γ_6 only in $\vec{E}\perp c$ orientation of the incident light.

Obviously, this inference gives the clue to analyze the observations. If the final state in the $\Gamma_8\ {}^4A_2(F) \rightarrow \Gamma_6\ {}^4T_1(P)$ absorption of Co^{2+} in $\bar{T}_d$ is degenerate with the quasicontinuum of conduction-band states involved in the charge-transfer process (i), and if we postulate the Co^{2+} ground state to be of Γ_5, Γ_6 type in the C_{3v} axial distortion, then only the $\vec{E}\perp c$ component of the internal transition, which originally has no polarization preference, will experience the antiresonant interaction. Hence, by means of process (i) not only an unconstrained explanation of the "positive dip" emerges but also the position of the Co^{2+} ground state is fixed in a distance of $13\,800 \pm 300$ cm^{-1} from the bottom of the conduction band. Both conclusions are in an overall agreement with the observations of Ref. 13.

Qualitatively, the d^7 level scheme is suitable to interpret the splitting behavior of the ${}^4F \rightarrow {}^4P$ transitions of Co^{2+}. There are, however, some difficulties concerning the quantitative determination of the spin-orbit (so) coupling parameter λ. The total splitting of the ${}^4T_1(P)$ level by so coupling is $\Delta\bar{\nu} \simeq 1350$ cm^{-1} (see Table I); this should, according to the static crystal-field theory, correspond to a value of $4\,|\,\lambda\,|$. Hence, $\lambda \simeq -350$ cm^{-1}, which is almost twice the value for the free Co^{2+} ion [$\lambda_0 = -178$ cm^{-1} (cf. 14)]. This discrepancy occurs with the Co^{2+} ion in other II-VI compounds as well (e.g., 15) and cannot, up to now, be explained. Owing to the low phonon energies in CdSe ($\hbar\omega < 220$ cm^{-1}, see Table II) an alternative interpretation of the triplet by phonon coupling is also out of question.

The transition ${}^4T_2(F) \rightarrow {}^4A_2(F)$ of the Co^{2+} ion has been known to be accompanied with emission in other II-VI compounds, e.g., ZnS and CdS (cf., for instance Refs. 11 and 21). Therefore, those CdSe crystals which display the absorption of Fig. 3 were searched for any luminescence in the spectral region around $\lambda = 3$ μm. In fact, a Co^{2+} emission is detected (Fig. 4) which is characterized at low temperature by a zero-phonon line at $\bar{\nu} = 2867$ cm^{-1}. It is followed by a vibronic side wing whose main peak is at 2824 cm^{-1}. Thus, a characteristic eigenfrequency of about 43 cm^{-1} occurs which is similar to the value at CdSe:Fe^{2+} found here (cf. Table I). This emission has been sought, but not found, by Radlinski,[11] who attributes its absence to a degeneracy of ${}^4T_2(F)$ with the conduction band. According to our findings on the above-discussed ${}^4A_2(F) \rightarrow {}^4T_1(P)$ absorption and to Baranowski *et al.*,[13,15] however, only the components of ${}^4P$ (and higher levels) are degenerate with the conduction

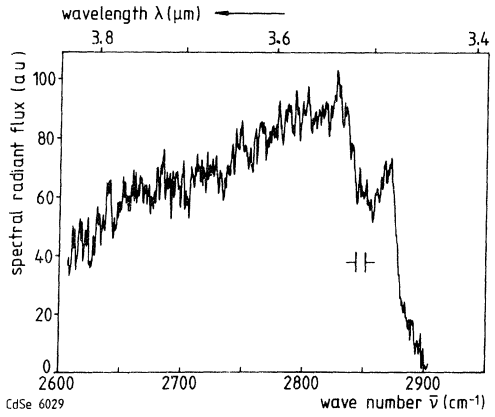

FIG. 4. Luminescence of a CdSe:Co^{2+} crystal (no. 6029) at $T \cong 4$ K. ${}^4T_2(F) \rightarrow {}^4A_2(F)$ transition. Cooled PbSe detector with Ge filter. Range of excitation: 7500 cm^{-1} $\lesssim \bar{\nu} \lesssim$ 15 000 cm^{-1}.

band. Therefore, in agreement with our results, the $^4T_2(F) \rightarrow {}^4A_2(F)$ transition is radiative.

The forbidden transition $^4T_2(F) \rightarrow {}^4A_2(F)$ is turned into an allowed one by spin-orbit coupling, because the inner Kronecker products of the representations of the simple group T_d with Γ_8 of the double group $\bar{T}_d$ must be formed to allow for the spin $S=\frac{3}{2}$. In doing so, T_2 splits like T_1 so that now, between the resulting Γ_6, Γ_7, and Γ_8 components of T_2 and the Γ_8 ground state, all transitions are allowed in absorption and emission.

C. Nickel (Ni^{2+})

In the absorption spectrum of CdSe:Ni^{2+} all the expected crystal-field transitions occur, viz., from the $^3T_1(F)$ ground state to the $^3T_2(F)$, $^3A_2(F)$, $^1T_2(D)$, and $^3T_1(P)$ levels.[1] Although no zero-phonon structures were resolved at $T \simeq 80$ K it could already be concluded[1] that the static crystal-field theory can only interpret the general splitting pattern of the energy levels, not even the relatively rough structural details in these spectra could be explained.

Now for the first time a sharply structured spectrum is found for the absorption transition $^3T_1(F) \rightarrow {}^3T_1(P)$, i.e., in the region around $\bar{\nu} \simeq 11\,000$ cm^{-1}, at $T \simeq 2$ K. The resolved zero-phonon transitions are partly polarized (Fig. 5) as could be expected for a substitutional Ni^{2+}_{Cd} ion in C_{3v} symmetry. Except for the cobalt transition at 14 175 cm^{-1}, the other previously treated processes did not require the inclusion of axial fields, partly because it was not possible to secure polarization phenomena with their faint spectral structures. A schematic splitting diagram for the ^3P term of the Ni^{2+} ion is also given in Fig. 5 where the T_d crystal-field, the spin-orbit, and the axial field (C_{3v}) contributions are considered successively. (The spin-orbit components have in this case been appointed in Mulliken's notation because the Γ_i labels were reserved for the irreducible representations of C_{3v}.) In C_{3v}, five transitions are allowed for the electric dipole operator from the Γ_1 ground state, whereas in T_d it was only A_1-$^3T_1(F) \rightarrow T_2$-$^3T_1(P)$. The transmission curves in Fig. 5 display clearly a doublet α_1-α_2 at $\bar{\nu} =$ 10926-10931 cm^{-1} which is strongly but not totally polarized and a number of further less pronounced transitions, see also Table III.

The corresponding emission spectrum of the same crystal in this region (Fig. 6) starts out with a

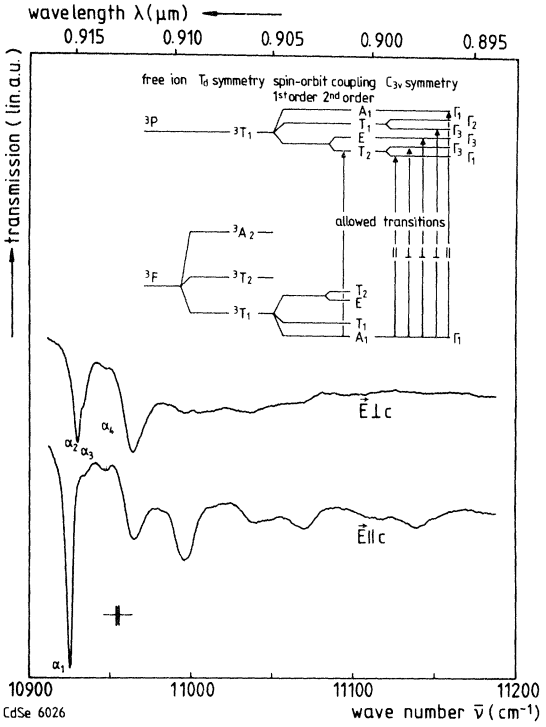

FIG. 5. Transmission spectrum of a CdSe:Ni^{2+} crystal (no. 6026) at $T \cong 2$ K and relevant part of the splitting scheme of the energy levels of the $3d^8$ electron configuration in T_d and C_{3v} crystal fields, respectively. The spectra for the $\vec{E} \| c$ and $\vec{E} \perp c$ orientations have been shifted vertically to avoid overlap. The plot is linear in transmission. In the main line α_1 at $\bar{\nu} = 10\,926$ cm^{-1} in $\vec{E} \| c$, the residual transmission is about 30%. Grating blazed near 6200 cm^{-1}, used in second order. Cooled photomultiplier (EMI type 9684B) with $S1$ photocathode.

narrow line near $\bar{\nu} = 10\,926$ cm^{-1}, which is accompanied by a series of subsidiary peaks superimposed on a broad vibronic band. The annexed luminescence structure at wave numbers $\nu \lesssim 10\,200$ cm^{-1} will be dealt with in Sec. III E. The coincidence between the zero-phonon lines in absorption and emission can be derived by comparing Figs. 5 and 6. It can be verified additionally by the appearance of a pronounced self-absorption in the emission spectrum of more strongly activated specimens. This is especially so in polarized emission scans which are not shown here. For instance, in the luminescence of crystal no. 6026, a dip is superimposed onto the 10 926-cm^{-1} line so that it assumes a doublet structure in the $\vec{E} \| c$ polarization. This effect is observed on exciting the crystal from the "rear" surface, that is, the one which is averted from the entrance slit of the monochromator. Consequently, for such crystals the undisturbed

TABLE III. Absorption and emission peaks of Ni^{2+} in CdSe crystal no. 6026. In some cases, where the relevant structure could be more distinctly resolved with other crystals, the line positions have been derived by averaging measurements on several crystals. All data in vacuum wave numbers (cm^{-1}).

Emission	Absorption	Polarization	Shift relative to zero-phonon line. $\Delta\bar{\nu}$ (cm^{-1})	Interpretation (see text) (I)	(II)
		(i) $^3T_1(F)\leftrightarrow{}^3T_1(P)$ band			
10702		||	−224	α_1-LO	
10730			−196		
10752			−174		
10781			−145		
10810		||	−116	α_1-LA	
10840		||	−86		
10865		||(⊥)	−61	α_1-TA	
10898		||(⊥)	−28	α_1-$\hbar\omega_3$	
10926	10926	||	±0	α_1	α_1
	10931	⊥	5	α_2	α_2
	10934	(||)⊥	8	α_3	α_3
	10948	||(⊥)	22	α_4	α_4
	10966	||⊥	40	$\alpha_1+\hbar\omega_1$	α_5
	10997	||	71	$\alpha_1+\hbar\omega_2$	$\alpha_1+\hbar\omega_2$
	11040	||⊥	114	α_1 + LA	$\alpha_5+\hbar\omega_2$
	11070	||	144	$\alpha_1+2\hbar\omega_2$	$\alpha_1+2\hbar\omega_2$
	11113	||	187		
	11139	||	213	α_1+LO	$\alpha_1+3\hbar\omega_2$
	11187		265		$\alpha_5+3\hbar\omega_2$
	11225		303		
	11274		352	α_1+2TO	
		(ii) $^3T_1(F)\leftrightarrow{}^3A_2(F)$ band			
	7472		0		
	7519		47		
	7588		116		
	7650		178		
	(iii) $^3T_1(F)\leftrightarrow{}^3T_2(F)$ band				
3607	3607		0		
	3646		39		
	3700		93		

zero-phonon structure must be obtained by excitation of the "front" surface. Crystals with random Ni doping exhibit, in general, the same spectral features but with lesser clarity, e.g., only about four vibronic side peaks. To sum up, the transition $^3T_1(P)\leftrightarrow{}^3T_1(F)$ is detected with CdSe in emission as well as in absorption.

Trying to interpret, as Langer and Baranowski[1] did, the structure of the $^3T_1(F)\rightarrow{}^3T_1(P)$ transition with static crystal-field theory on inclusion of only the first-order spin-orbit interaction, the difficulties arise which were already reported by these authors. The resulting spin-orbit coupling constant $\lambda \cong -380\ cm^{-1}$ compared to $\lambda_0\cong -325\ cm^{-1}$ of the free Ni^{2+} ion[14] would be too large. Using this model for an interpretation of our absorption data, $\alpha_1-\alpha_4$ [see Table III, interpretation (II)] would have to be regarded as transitions to components of T_2-$^3T_1(P)$. It would be impossible to interpret the splitting and polarization behavior of these lines by axial terms in the crystal field. α_3 and α_4 could perhaps be ascribed to structural lattice defects. The line α_5, shifted by $\Delta\bar{\nu}\cong 40\ cm^{-1}$, would be the forbidden A_1-$^3T_1(F)\rightarrow E$-$^3T_1(P)$ transition. The doublet α_1-α_5 split by second-order spin-orbit coupling would reoccur threefold in the spectrum, shifted by $\Delta\bar{\nu}\cong 71\ cm^{-1}$, possibly due to coupling of a reduced acoustic CdSe phonon.

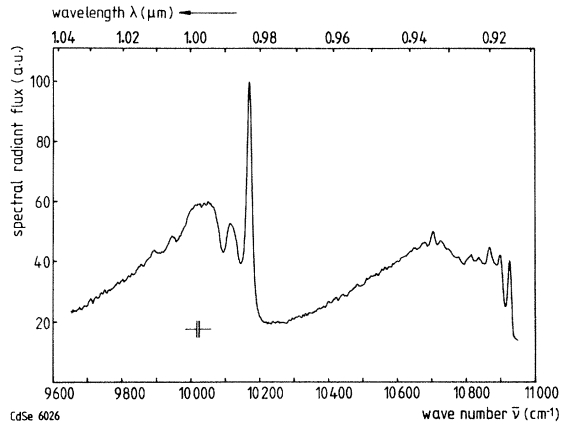

FIG. 6. Emission spectrum of a CdSe crystal (no. 6026) at $T=4$ K. In the 9600 $cm^{-1} \lesssim \bar{\nu} \lesssim 10200$ cm^{-1} region, an emission is displayed, which is tentatively related to an M center, in the 10200 $cm^{-1} \lesssim \bar{\nu} \lesssim 11000$ cm^{-1} region, the ${}^3T_1(P) \rightarrow {}^3T_1(F)$ transition of Ni^{2+} appears. Range of excitation: 15500 $cm^{-1} \lesssim \bar{\nu} \lesssim 30000$ cm^{-1}. Grating blazed near 6200 cm^{-1}, used in second order. Cooled PbS detector. Corrections have been made for grating efficiency, detector response, and change of abscissa. Some residual first-order background.

With regard to the many discrepancies in these considerations, we favor the interpretation of the ${}^3T_1(F) \rightarrow {}^3T_1(P)$ transition in terms of a model suggested by Kaufmann and Koidl[22] for ZnS:Ni where the electron-phonon interaction is considered. We did not explicitly repeat these calculations for CdSe:Ni but we can suggest an interpretation of our data based upon analogy conclusions [cf. Table III, interpretation (I)]. The proposed interpretation is, by the way, further corroborated by a recent study of the Zeeman splitting of the corresponding ${}^3T_1(F) \rightarrow {}^3T_1(P)$ absorption lines in $CdS:Ni^{2+}$.[23]

Owing to electron-phonon interaction it is possible that the "zero-phonon states" T_2, E, T_1, and A_1 of ${}^3T_1(P)$ mix with the "single-phonon states" T_2', E', T_1', and A_1', or higher excited states. Hence, so-called quasi-zero-phonon states result whose energy distances are changed considerably compared to the static case. As has been shown in Ref. 22, even with consideration of this electron-phonon interaction, again the quartet T_2, E, T_1, and A_1 occurs. The energy differences are, however, reduced by a factor of about 10, i.e., there is a strong reduction of the spin-orbit coupling parameter λ. Moreover, the levels T_1 and A_1 can, at suitable mode coupling, interchange, and finally, also the phonon energies are reduced in coupling to these terms.

We ascribe the first four absorption lines ($\alpha_1 - \alpha_4$) to such a reduced spin-orbit quartet. Based on the observed polarization properties it can be concluded that the "natural" sequence of the quartet (T_2, E, T_1, and A_1) is maintained. The polarization properties can be derived by considering the trigonal field. However, the C_{3v} splitting of the transition α_1, i.e., A_1- ${}^3T_1(F) \rightarrow$ T_2- ${}^3T_1(P)$, is not resolved due to its smallness (the C_{3v} splitting is about 1 or 2 orders of magnitude smaller than the spin-orbit splitting).

The phonon satellites in absorption (Fig. 5) can be interpreted partly by reduced phonons and partly by intrinsic CdSe phonons. The first secondary maximum at $\bar{\nu} = 10966$ cm^{-1} is produced by a reduced TA phonon (see Tables II and III), the second secondary maximum at $\bar{\nu} = 10997$ cm^{-1} by a reduced LA phonon. The reduction is 35% in both cases. The polarization of the secondary maxima can be interpreted by the selection rules for phonon coupling, i.e., TA excitation is favored in $\vec{E} \perp c$ orientation and LA in $\vec{E} \parallel c$. The following secondary maxima cannot definitely be assigned; both multiples of the reduced acoustic phonons and optical phonons can couple (see Tables II and III). The secondary maxima found in Ref. 1 in the region up to $\bar{\nu} \cong 12500$ cm^{-1} at $T=80$ K, which were attributed to a splitting by spin-orbit coupling, would, according to our model, have to be ascribed rather to transitions into singlet terms, as they have also been found[24] with $ZnS:Ni^{2+}$.

With unintentionally Ni-doped crystals, in emission only four or five phonon satellites of the zero-phonon line occur; at the deliberately doped crystals there are, however, more. The maxima of the weakly doped crystals agree with the pronounced peaks of the strongly doped crystals (cf. Fig. 6). As stated before in discussing the absorption satellites, in the emission spectrum, too, in addition to the prominent LO-phonon satellite at 10702 cm^{-1}, energy differences have been observed which cannot be ascribed to any of the pure lattice phonons. This could be expected because of the Jahn-Teller coupling observed in absorption. A definite conclusion on the influence of the Jahn-Teller effect in emission cannot be drawn as yet; indeed, the measured phonon energies are generally different for absorption and emission so that a different lattice coupling must be expected in the ground and excited states, respectively.

In the mentioned paper,[1] the absorption bands at 80 K which correspond to transitions from the

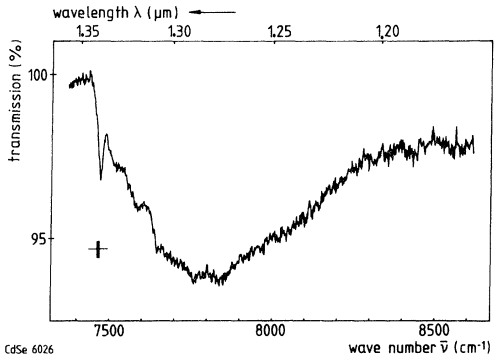

FIG. 7. Transmission spectrum of a CdSe:Ni^{2+} crystal (no. 6026) at $T \cong 2$ K in the region of the $^3T_1(F) \rightarrow {}^3A_2(F)$ absorption. Grating blazed near 6200 cm^{-1}, used in first order. Cooled PbS detector.

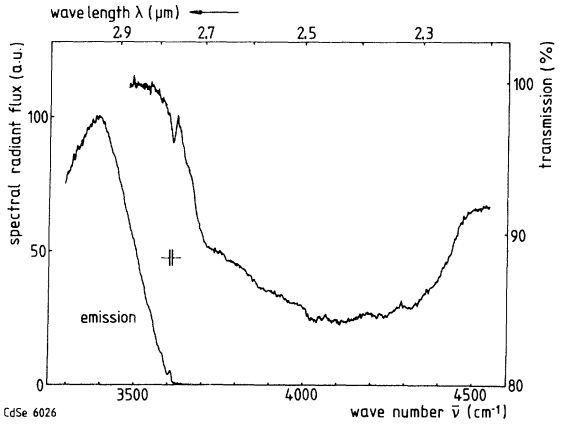

FIG. 8. Emission and transmission spectrum of a CdSe:Ni^{2+} crystal (no. 6026) at $T = 2$ K in the region of the $^3T_1(F) \rightarrow {}^3T_2(F)$ absorption transition. Excitation range in the emission experiment: 16 600 $cm^{-1} \lesssim \tilde{\nu} \lesssim$ 28 500 cm^{-1}. Grating blazed near 3850 cm^{-1}, used in first order. Cooled PbS detector. The same corrections were applied as in Fig. 6.

$^3T_1(F)$ ground state to the other components of ^3F, i.e., $^3T_2$ and $^3A_2$ (cf. inset of Fig. 5), were also reported. In particular, $^3A_2(F)$ gives rise to a broad band between 7400 and 8600 cm^{-1} at liquid-nitrogen temperature. Lowering the temperature reveals here a zero-phonon line at $\bar{\nu} = 7472$ cm^{-1} and several satellite structures on the annexed absorption band (Fig. 7 and Table III). A search for a corresponding transition in emission indicated a band in the adjacent 7000–7500-cm^{-1} range; a high-resolution experiment could, however, not be realized due to filtering difficulties. It proved to be impracticable to suppress strong second-order radiation from the 13 000–15 000 cm^{-1}-edge emission-exciton region. For this reason we are not able to present an emission spectrum of the $^3A_2(F) \rightarrow {}^3T_1(F)$ transition though it is radiative.

The lowest-energy absorption of Ni^{2+}, $^3T_1(F) \rightarrow {}^3T_2(F)$, arises at about 3900 cm^{-1} according to Ref. 1. Here, again, in the low-temperature transmission spectrum of a CdSe crystal, a distinct but weak zero-phonon line could now be resolved at the low-energy slope of the band at $\bar{\nu} = 3607$ cm^{-1} (Fig. 8). As for the rest, the course of the absorption spectrum is, however, poor in structure.

In emission, a corresponding line could be detected as a tiny peak at the brink of a broad band with a maximum at 3390 cm^{-1}. Hence, the $^3T_2(F) \rightarrow {}^3T_1(F)$ transition which is allowed in T_d symmetry is definitely radiative and is characterized here by a fairly well-pronounced lattice coupling. This same transition has recently been studied[24] in luminescence with ZnS:Ni^{2+} where a number of sharp lines could be resolved. The stated observations on CdSe:Ni^{2+} provide the first known example of a transition-metal ion in a II-VI semiconductor with more than one electronic transition from a crystal-field level to the ground state being radiative.

D. Vanadium

Whereas in absorption several crystal-field transitions have been observed[1] at vanadium centers in CdSe, in emission only one band has been detected.[25] This emission band is situated in the spectral region around 4500 cm^{-1} as in other II-VI compounds (cf. Ref. 26). The respective luminescence has been investigated by us recently[27] in CdS:V,Cu; in this host lattice, however, a further emission band appeared near 8500 cm^{-1}. In that paper[27] we concluded that in cadmium sulfide the investigated optical effects take place at the three-valent vanadium ion (d^2 configuration). The earlier measurements of other authors on CdSe:V are usually interpreted in a V^{2+} model (d^3). Most of the data are, however, lacking completeness, and interpretations were possible only with reservations.

In this study, with vanadium-doped CdSe crystals an emission band appears with a maximum near 4300 cm^{-1} at liquid-helium temperatures. This is the spectral region where Le Manh Hoang and Baranowski[25] also found an emission maximum at about 4 K. Taking as a basis the V^{3+} model, as in the case of CdS:V, the emission corresponds to the transition $^3T_2(F) \rightarrow {}^3A_2(F)$ (see Table

I). The additional transition $^3T_1(F) \rightarrow {}^3A_2(F)$ would be situated in CdSe:V^{3+} near $\bar{\nu} \cong 6000$ cm^{-1}. In this region, however, most of the available CdSe crystals exhibit the tail of a strong broad emission band peaking near 6500 cm^{-1}, which is probably due to copper. This band prevented a clear decision if the luminescence which we actually detected with vanadium-activated CdSe in this range was definitely related to V^{3+}. It is, therefore, still unclear whether the charge state V^{3+} or rather V^{2+} prevails in CdSe.

E. Further transitions

A new emission occurs near $\bar{\nu} \cong 10\,000$ cm^{-1} (see the left-hand part of Fig. 6 and Table I). We have observed this emission in all investigated crystals, but with differing relative spectral radiant intensity. The spectral position of the band seems to indicate at first glance that it may be the zero-phonon structure of the familiar[28] broad band near 8500 cm^{-1}. Various imperfections may be able to form the luminescent centers for the broad bands which often occur there in CdSe (cf. Refs. 29 and 30), so for example intrinsic defects[31] or a copper impurity.[32] The large interspace of the 10 170 cm^{-1} ZPL from the 8500-cm^{-1} band and the observed variations in the relative intensities of these structures as recorded with different crystals, however, render an association of these phenomena via phonon coupling rather improbable.

The external appearance of the novel emission structure is notable. It is commensurate for all investigated crystals, i.e., the ratios of the spectral intensities and the half-widths of the individual maxima are equal throughout. The first sharp line at $\bar{\nu} = 10\,170$ cm^{-1} which must obviously be ascribed to a zero-phonon transition is still rather broad (half-width $\Delta\bar{\nu} \cong 14$ cm^{-1}), it is preferentially polarized with $\vec{E} \perp c$. The first secondary peak is also broad (see Table I), not even with smaller spectral slit widths could it be resolved into components. We, therefore, assume that this emission involves an intrinsic lattice property, for instance, an imperfection or possibly a radiative charge-transfer transition involving some unspecified center. The spectral position, as mentioned above, also seems to suggest such an intrinsic defect.

Interestingly enough, a corresponding narrow absorption transition at the same place is missing. Several authors report, however, broad absorption effects in this region (cf. Ref. 1), sometimes measured in the photoconductivity spectra.[33,34] These features are usually attributed to charge transfer transitions at copper centers involving the release of electrons from the center to the conduction band. A connection with the described Ni^{2+} emission at 10 926 cm^{-1} is not plausible, since, firstly, the energy distance is larger than is the highest characteristic phonon energy, and secondly, the overall appearance of the bands is completely different. A pure transition-metal effect can fairly well be excluded anyway, since the spectral position does not correspond with the known positions of internal transition-metal absorption bands.

The spectral position and the spectral shape of the new luminescence suggest a tentative interpretation in terms of inner transitions of an M center, i.e., an associative defect comprising two adjacent anion vacancies each with positive effective charge: $(V_{Se}^{-}\, V_{Se}^{-})^{2+}$. The presence of this type of imperfection has recently been demonstrated for ZnS.[35] A transfer of the arguments given in that study starts from $a_1 = 0.43$ nm, the distance of Se neighbors in the hexagonal CdSe lattice. By means of an intermediate permittivity $\epsilon_m = (\epsilon_\infty + \epsilon^{1/2})/2$, an effective distance $R = a_1/\epsilon_m$ is calculated for the two positive charges of an H_2 molecular model and the resulting singlet-triplet transition energy $E(H_2)$ for this particular R value is then reduced by a factor of $\epsilon_{\text{eff}}^{-2} \cong \epsilon_\infty^{-1}$ to obtain the corresponding transitional energy for the solid.[36] In our case, with $\epsilon_\infty \cong 6.1$,[37] an $E(H_2) \cong 7.5$ eV is obtained from Ref. 38 which yields an estimate of $\bar{\nu}(M) \cong 10\,100$ cm^{-1} for the postulated M center in CdSe. Though the striking "accuracy" of this consideration is certainly merely incidental, one is encouraged to pursue the idea of an M center being involved.

The shape of the emission band of CdSe (cf. Fig. 6) resembles the M-center spectrum of ZnS indeed, provided that the pronounced fine structures in the ZnS spectrum are averaged to some extent, in the present case due to a lower structural purity of the CdSe crystals. The main line at 10 170 cm^{-1} should correspond to the main doublet near 11 950 cm^{-1} (lines 10 and 11) of ZnS, the main CdSe satellite near 10 120 cm^{-1} to the zero-phonon line 20 and the satellites 21 and 22 of ZnS. The shift $\Delta_1 \cong 50$ cm^{-1} (CdSe) compares with the 125-cm^{-1} shift of ZnS. The region from 1000 to 10 070 cm^{-1} in the present spectrum with surmised LA- and TO-phonon coupling seems to match with nos. 28–31 structures of ZnS and, finally, an LO satellite is prominent with CdSe ($\bar{\nu} = 9950$ cm^{-1}, cf. Table I) as with ZnS (lines 34, 35, and 37). To conclude, if the prevalence of Se vacancies in as-

grown CdSe is also considered, which has been demonstrated by a number of investigators,[39–41] an interpretation of the new luminescence band as an internal transition of *M* centers is the most likely hypothesis at present.

Some further broad emission bands have been observed in the spectral region $\bar{\nu} < 8000$ cm^{-1} with a number of crystals. They cannot, however, yet be ascribed definitely to specific impurities. This requires more detailed investigations.

IV. CONCLUSIONS

The data gained at low temperatures yield, in the case of the Fe^{2+}, Ni^{2+}, and Co^{2+} absorptions, remarkable new facts and allow a revision of some previous interpretations. For the first time, pronounced zero-phonon structures are observed for Fe^{2+}, Co^{2+}, and Ni^{2+}. In the case of the Fe^{2+} absorption, the energy position of the zero-phonon lines is revised. The too-high value of the spin-orbit coupling parameter λ was confirmed for Co^{2+}, the estimated splitting by second-order spin-orbit coupling is also new. Evidence for an autoionization effect related to the charge transfer $Co^{2+} \rightarrow Co^{3+}$ is presented by an analysis of a polarized transmission spectrum of CdSe:Co^{2+}. With the ${}^3T_1(F) \rightarrow {}^3T_1(P)$ transition at the Ni^{2+} center, for the first time, a Jahn-Teller effect can be inferred for an impurity center in CdSe. The spin-orbit coupling parameter λ is, due to electron-phonon interaction, strongly reduced.

In emission, apart from the known vanadium band, several novel bands have been measured which are partly caused also by transition metals. These are the Fe^{2+} emission at 2375 cm^{-1}, the Co^{2+} emission at 2867 cm^{-1}, and the Ni^{2+} emissions at 10926, around 7200 cm^{-1} and at 3607 cm^{-1}, as well as another emission band at 10170 cm^{-1}, which is tentatively related to an *M* center. Mostly, the luminescent bands exhibit zero-phonon structures which enabled us to supplement the findings which were obtained from absorption data for the involved imperfections.

ACKNOWLEDGMENTS

The authors wish to thank Dr. R. Broser of this institute, Dr. R. Lauck, Physikalisches Institut der Universität Karlsruhe, and Dr. D. C. Reynolds, Aerospace Research Labs, Ohio for supplying some of the crystals used here. Moreover, they are indebted to Frau L. Haussknecht for the vapor deposition of some crystals with vanadium. Parts of this paper are based upon the diploma work of D. Buhmann, Fachbereich Physik, Technische Universität Berlin, thesis advisors: Professor I. Broser and Professor H.-J. Schulz.

[1]J. M. Langer and J. M. Baranowski, Phys. Status Solidi 44, 155 (1971).
[2]G. Grebe and H.-J. Schulz, Z. Naturforsch. 29a, 1803 (1974).
[2]G. Grebe and H.-J. Schulz, Z. Naturforsch. 29a, 1803 (1974).
[3]W. Low and M. Weger, Phys. Rev. 118, 1119 (1960); 118, 1130 (1960); 120, 2277 (1960).
[5]F. S. Ham and G. A. Slack, Phys. Rev. B 4, 777 (1971).
[6]G. A. Slack, Phys. Rev. B 6, 3791 (1972).
[7]V. P. Srivastava and G. S. Verma, Phys. Rev. B 10, 219 (1974).
[8]G. F. Koster, J. O. Dimmock, R. G. Wheeler, and H. Statz, in *Properties of the Thirty-Two Point Groups* (MIT, Cambridge, Mass., 1963).
[9]C. H. Henry, K. Nassau, and J. W. Shiever, Phys. Rev. B 4, 2453 (1971).
[10]I. Filinski and B. Wojtowicz-Natanson, J. Phys. Chem. Solids 32, 2409 (1971).
[11]A. P. Radlinski, J. Phys. C 12, 4477 (1979).
[12]J. M. Baranowski, J. M. Noras, and J. W. Allen, J. Phys. C 7, 4529 (1974).
[13]J. M. Baranowski, J. M. Langer, and S. Stefanova, in *Proceedings of the Eleventh International Conference on the Physics of Semiconductors,* edited by M. Miasek (PWN Polish Scientific, Warsaw, 1972), Vol. II, p. 1001.
[14]J. S. Griffith, *Theory of Transition-Metal Ions* (Cambridge University Press, Cambridge, 1961).
[15]J. M. Baranowski, J. W. Allen, and G. L. Pearson, Phys. Rev. 160, 627 (1967).
[16]R. Geick, C. H. Perry, and S. S. Mitra, J. Appl. Phys. 37, 1994 (1966).
[17]R. Beserman, Ann. Phys. (France) 4, 197 (1969).
[18]V. G. Plotnichenko, Yu. A. Mityagin, and L. K. Vodopyanov, Fiz. Tverd. Tela (Leningrad) 19, 2706 (1977) [Sov. Phys.—Solid State 19, 1584 (1977)].
[19]T. Fukumoto, H. Yoshida, S. Nakashima, and A. Mitsuishi, J. Phys. Soc. Jpn. 32, 1674 (1972).
[20]P. Y. Yu, Solid State Commun. 19, 1087 (1976).
[21]H.-E. Gumlich and H.-J. Schulz, J. Phys. Chem. Solids 27, 187 (1966).
[22]U. G. Kaufmann and P. Koidl, J. Phys. C 7, 791

(1974).
[23]I. Broser, R. Germer, and H.-J. Schulz, Phys. Status Solidi B 101, 181 (1980).
[24]G. Roussos and H.-J. Schulz, Phys. Status Solidi B 100, 577 (1980).
[25]Le Manh Hoang and J. M. Baranowski, Phys. Status Solidi B 84, 361 (1977).
[26]M. Avinor and G. Meijer, J. Phys. Chem. Solids 12, 211 (1960).
[27]D. Buhmann, H.-J. Schulz, and M. Thiede, Phys. Rev. B 19, 5360 (1979).
[28]M. Avinor and G. Meijer, Chem. Phys. 32, 1456 (1960).
[29]G. L. Belenkii, A. V. Lyubchenko, and M. K. Sheinkman, Fiz. Tekh. Poluprovodn. 2, 540 (1968) [Sov. Phys.—Semicond. 2, 445 (1968)].
[30]G. L. Belenkii, I. B. Ermolovich, N. B. Lukyanchikova, and M. K. Sheinkman, Fiz. Tverd. Tela (Leningrad) 9, 3337 (1967) [Sov. Phys.—Solid State 9, 2626 (1968)].
[31]H.-J. Schulz and B. A. Kulp, Phys. Rev. 159, 603 (1967).
[32]R. E. Halsted, M. Aven, and H. D. Coghill, J. Electrochem. Soc. 112, 177 (1965).
[33]V. E. Mashchenko, A. G. Gusachenko, V. M. Vantsan, and B. M. Bulgakov, Zh. Prikl. Spektrosk. 23, 855 (1975).
[34]M. A. Rizakhanov, G. M. Gasanbeko, and V. T. Krongauz, Fiz. Tekh. Poluprovodn. 12, 993 (1978) [Sov. Phys.—Semicond. 12, 589 (1978)].
[35]I. Broser, R. Germer, F. Seliger, and H.-J. Schulz, J. Phys. Chem. Solids 41, 101 (1980).
[36]R. Herman, M. C. Wallis, and R. F. Wallis, Phys. Rev. 103, 87 (1956).
[37]H. W. Verleur and A. S. Barker, Jr., Phys. Rev. 155, 750 (1967).
[38]G. Herzberg, in *Spectra of Diatomic Molecules* (Van Nostrand Reinhold, New York, 1950).
[39]H. Tubota, Jpn. J. Appl. Phys. 2, 259 (1963).
[40]F. T. J. Smith, Solid State Commun. 8, 263 (1970).
[41]A. Sakalas and R. Baubinas, Phys. Status Solidi A 31, 301 (1975).